The Predictive Power of Computational Astrophysics as a Discovery Tool
Proceedings IAU Symposium No. 362, 2023
D. Bisikalo, D. Wiebe & C. Boily, eds.
doi:10.1017/S1743921322001569

Numerical modelling of X-shaped radio galaxies using back-flow model

Gourab Giri and Bhargav Vaidya

Department of Astronomy, Astrophysics and Space Engineering, Indian Institute of Technology Indore, Simrol 453552, Madhya Pradesh, India
emails: gourab@iiti.ac.in, bvaidya@iiti.ac.in

Abstract. The focus of this work is to comprehensively understand hydro-dynamical back-flows and their role in dynamics and non-thermal spectral signatures particularly during the initial phase of X-shaped radio galaxies. In this regard, we have performed axisymmetric (2D) and three dimensional (3D) simulations of relativistic magneto-hydrodynamic jet propagation from tri-axial galaxies. High-resolution dynamical modelling of axisymmetric jets has demonstrated the effect of magnetic field strengths on lobe and wing formation. Distinct X-shape formation due to back-flow and pressure gradient of ambient is also observed in our 3D dynamical run. Furthermore, the effect of radiative losses and diffusive shock acceleration on the particle spectral evolution is demonstrated, which particularly highlights how crucial their contributions are in the emission signature of these galaxies. This imparts a significant effect on the galaxy's equipartition condition, indicating that one must be careful in extending its use in estimating other parameters, as the criterion evolves with time.

Keywords. Galaxies: jets, Acceleration of particles, Magnetohydrodynamics (MHD), Methods: numerical

1. Introduction

Extended radio galaxies have radio jets that emanate from the central Active Galactic Nuclei (AGN) and travel along a route specified by the central black hole's spin axis. Some of these radio galaxies show significant distortion in their jet forming winged radio sources. They can be identified by observing the presence of two double lobe structures aligned at an angle to each other (forming X-shape) (Kraft et al. 2005). Due to this peculiarity, several formation mechanisms have been attributed to describe its formation process along with their plausible support from low frequency radio observations (see Gopal-Krishna et al. 2012). However, to date there exists no general agreement between the proposed models. Here, we will study the Back-flow model (Leahy Williams 1984; Capetti et al. 2002) as the possible origin of X-morphology using numerical simulations. As per the Back-flow model, back flow of jet material formed as a result of the pressure imbalance at the jet head are strongly deflected by the ambient medium itself, forming an X-shaped source. Several simulation studies have already been conducted in this regard, addressing numerous dynamical characteristics of the synthetic morphology having X-shape (Hodges-Kluck & Reynolds 2012; Rossi et al. 2017). However, in terms of their emission modelling, these studies have used rather proxies (i.e. pressure as emissivity) or a simplistic treatment of it ignoring the crucial effect of several micro-physical processes (e.g. cooling and re-energization processes) on particle spectral upgradation and hence on the emission.

In this work, we are intending to address some of the fundamental aspects of the Back-flow model, and explore its associate signatures on the appeared morphology. Then, we plan to describe the spectral aspect of these radio galaxies by accurately incorporating the effects of ongoing micro-physical processes like radiative and adiabatic losses, as well as the particle re-energization process due to diffusive shocks. This allows us to track the spectral history of emitting particles throughout the galaxy, and investigate how much crucial re-energization processes are in keeping the structure active, allowing us to distinguish between distinct formation mechanisms.

2. Simulation Setup

Our numerical simulations were performed using the relativistic magneto-hydrodynamic (RMHD) module of PLUTO code (Mignone et al. 2007).

• **Dynamical modelling:**

We have initialized a tri-axial ellipsoidal galaxy medium using the King's density profile (Cavaliere & Fusco-Femiano 1976) defined (in Cartesian system) as

$$\rho = \frac{\rho_0}{(1 + x^2/a^2 + y^2/b^2 + z^2/c^2)^{\frac{3}{4}}} \tag{2.1}$$

where ρ_0 is the central density of the galaxy (1 amu/cc) and a, b and c are the effective core radii (4/3, 8/3 and 1 kpc respectively). The galaxy posses an initial isothermal atmosphere, static equilibrium of which is maintained by a gravity profile that is obtained using the hydro-static equilibrium equation. At the centre of this distribution, we have introduced a jet nozzle which will continuously inject bi-directional relativistic jet (radius 200 pc) having Lorentz factor $\Gamma = 5$ and which is under-densed as $10^{-6}\rho_0$. A toroidal B-field in the jet injection region is incorporated which is defined as $B_x = -B_t r sin\vartheta$ and $B_y = B_t r cos\vartheta$ where r and ϑ are the polar coordinates in the perpendicular plane to the jet ejection axis and B_x, B_y are the components of the field defined in that plane. The value of B_t is constant and is determined through the jet magnetization parameter σ (set to 0.01) which is the ratio of Poynting flux to the matter energy flux ($\frac{B_t^2}{\Gamma^2 \rho h}$; h is the specific enthalpy). To be specific, we have followed the initial configuration of Rossi et al. (2017) in modelling the dynamics of X-shaped radio galaxies (XRGs), focusing on their early formation phase in a galactic medium (i.e. evolution up to 4 Myr).

• **Spectral modelling:**

Additionally, we have used the hybrid framework of the PLUTO code, which helps us inject Lagrangian macro-particles into the domain, to model the spectral properties of these galaxies (Vaidya et al. 2018; Mukherjee et al. 2021). We continuously inject these particles with the jet in order to fill the computational domain with $\sim 10^6$ particles by the end of the simulation. Each macro-particle represents an ensemble of non-thermal electrons which follows a power law pattern (initially) defined as $N(\gamma) = N_0 \gamma^{-p}$ with index $p = 6$. The value of N_0 can be obtained by $\int_{\gamma_{\min}}^{\gamma_{\max}} N(\gamma) d\gamma = n_{\rm micro}$ where $n_{\rm micro}$ is the non-thermal electron number density. Its value is set by assuming that the energy density of the injected electrons (U_e) is a fraction of the magnetic energy density $\left(\frac{B_{\rm dyn}^2}{8\pi}\right)$ at the injection region, i.e. (in cgs units)

$$U_e = m_e c^2 \int_{\gamma_{\min}}^{\gamma_{\max}} \gamma N(\gamma) d\gamma \left(= \frac{B_{\rm eq}^2}{8\pi}\right) = \epsilon \frac{B_{\rm dyn}^2}{8\pi} \tag{2.2}$$

The equipartition magnetic energy density is represented by the term in the bracket in Eq. (2.2) (Hardcastle et al. 2002). In reality, $B_{\rm eq}$ (the equipartition magnetic field) is rather a proxy for magnetic field defined such that magnetic energy associated is equivalent to the radiating electrons energy and therefore cannot be considered as physical

https://doi.org/10.1017/S1743921322001569 Published online by Cambridge University Press

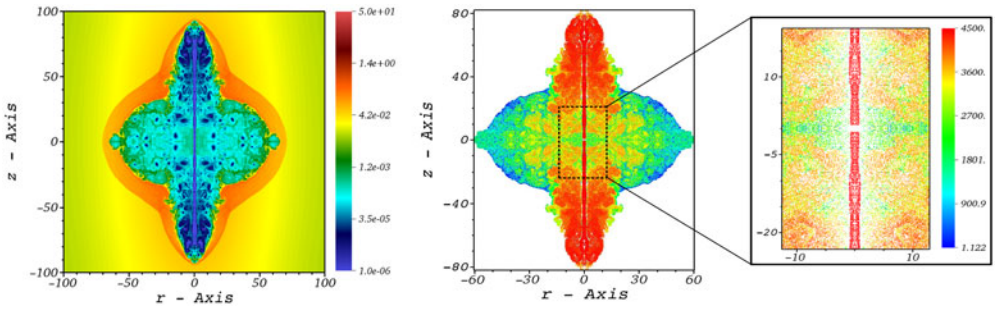

Figure 1. *Left:* density distribution of the galaxy, obtained from our 2D-run, is shown at time 3.26 Myr. *Right:* distribution of the Lagrangian macro-particles injected into the domain where the associate color bar represents the time of their injection. A higher value of it indicates a freshly injected plasma which suggests that the accumulation of older particles occurs in the wings. A zoomed version of this map represents the particle injection process from the central injection region i.e. the jet nozzle. Here length, density and time are defined with respect to 200 pc, 1 amu/cc and 651.8 yrs respectively.

magnetic field. Here, ϵ represents the fraction which is set to the value of 2.7×10^{-4} under the limiting Lorentz factors 10^2 ($\gamma_{\rm min}$) and 10^{10} ($\gamma_{\rm max}$) of the electrons. The choice of ϵ is rather arbitrary, resulting in a sub-equipartition strength of emission with $B_{\rm eq} = 0.01 B_{\rm dyn}$. Hence, we obtain the value of $n_{\rm micro}$ as $10^{-3}\rho_j$ where ρ_j is the jet density. The initial spectral distribution of the electrons will be modified over time depending on the micro-physical processes it undergoes like radiative losses, adiabatic cooling or diffusive shock acceleration which we considered in our simulations. For this reason, the particles are insensitive to the initial conditions when they travel some distance away from the injection region. The radiative losses considered here are the synchrotron and the inverse Compton (IC-CMB) emission.

We simulate a 3D Cartesian domain having size $(16 \times 32 \times 16)$ kpc, distributed in $192 \times 384 \times 192$ grids. We note here that a simpler version of this model in 2D is also performed by us in sufficiently high resolution (1536×1536 grids for (20×20) kpc domain) to understand the formation of X-morphology and effect of Back-flow on the morphological signature (in high resolution). The simulation was conducted in cylindrical geometry in $r - z$ plane (axisymmetric run) where z-axis represents the major axis of the galaxy (in 3D setup, it is the y-axis).

3. Formation of X-shaped morphology

The result of our simulation has been highlighted in Fig. 1, where in the left panel, the density distribution of the galaxy at time 3.26 Myr is represented (obtained from the 2D run). The strong bow shock and the contact discontinuity of the cocoon formed due to the jet-ambient interaction are highlighting a distinct X-shape of the galaxy where the jet is travelling along the major axis of the ambient. In this case, the over-pressured cocoon, formed due to the the continuous inflation of back-flowing material from jet, expands rapidly along the maximum pressure gradient path of the galaxy i.e. along the minor axis of the tri-axial medium. The high resolution map also shows the formation of several turbulent features in the cocoon, especially also in the wings, which play a crucial role in influencing the emission aspect of these structures via re-energization (discussed later). In the right part of Fig. 1, we show the particle distribution map of the galaxy where the associate colorbar represents the time of their injection into the domain. A higher value of injection time indicates a freshly injected particle. From figure, it is evident that the accumulation of older particles occurs in the wings, whereas the active lobes

https://doi.org/10.1017/S1743921322001569 Published online by Cambridge University Press

are filled with fresh plasma, satisfying the basic prediction of the Back-flow model. The zoomed version of this map represents the continuous particle injection process from the jet nozzle where the recollimations of jets are visible. We observed that the prominence of the formed X-shape reduces with the increasing angle between the major axis of the galaxy and the jet ejection axis (as typically observed), indicating the crucial role of ambient medium in shaping these morphologies.

The observed shape of the structure is however sensitive to the initial value of the magnetic field in the jet. A higher value of B-field is capable of suppressing the extent of the wing which in turn make the lobe expansion faster leading it to form a classical radio galaxy, even though it travels along the major axis of a highly elliptical ambient medium. Whereas, a weaker value of it will increase the prominence of the formed X-shape. The average B-field value at the end of the simulation for 2D-case is found to be several time higher than the values obtained in our 3D runs. This is due to the dimensional restriction of the cocoon expansion as the simulation has been carried out in 2D. As a result of which, the cocoon becomes incapable of reducing the B-field values that in turn affect the emission signature of the galaxy as well (as the particles cool down faster).

The basic characteristics described above, also hold true in our 3D run, however due to no dimensional restrictions, the structure evolve self consistently there (Fig. 2). For our further quantitative analysis, we will now focus on the results obtained from our 3D simulation.

4. Diffusive shock and equipartition condition

While determining the strength of the magnetic field from observation of synchrotron radiation of radio galaxies, it is mostly assumed that the radiating electrons are in equipartition with the magnetic energy of the cocoon. The equipartition condition is written in Eq. 2.2. However, several studies based on the IC-CMB measurement or the analytical modeling of radio galaxies have shown an overestimated value of $B_{\rm eq}$ compared to its actual value ($B_{\rm dyn}$) (Croston et al. 2005; Kraft et al. 2005; Mahatma et al. 2020).

Using the Lagrangian macro-particles injected into the domain, we have intended here to verify the evolution of equipartition condition of the simulated XRG (in 3D). The particles injected into the domain have started with a sub-equipartition strength as discussed in Section 2. Subsequently, we see that the condition is getting updated for the particles as they undergo through the micro-physical processes considered in the simulation. In this regard, we have tracked four particles injected into the domain at different times and plotted the ratio of the equipartition B-field strength ($B_{\rm eq}$) to the dynamical B-field strength ($B_{\rm dyn}$), where $B_{\rm eq} = B_{\rm dyn}$ indicates true equipartition. The trajectories of these particles are plotted in the top panel of Fig. 2 over the 2D slice of the formed X-shaped structure at 3.78 Myr (for visualisation and) to show where the particles end up at 3.78 Myr. In the bottom panel, the corresponding evolution of magnetic field ratios (i.e. $B_{\rm eq}/B_{\rm dyn}$) are shown for these particles. From figure, we can observe that all the particles are showing an overall increasing nature of the B-field ratio with time from their initial phase marked by the dashed grey line. The primary causes of this growth are as follows: (a) the particles are subjected to diffusive shocks at the shock locations that they encounter in their trajectory, and (b) the adiabatic expansion of the cocoon leading to a subsequent decrease of $B_{\rm dyn}$ field strength. We observed that the strength of these shocks varies between compression ratio values of 1.2 to 4 that correspond to weakest to strongest shocks, which further hints that shock re-acceleration plays a crucial role in updating the particle spectra and hence the emission of these galaxies. These shocks put a temporary hold on the drastic cooling of particles, and as a consequence the spectra will be flatter than expected from spectral ageing. An imprint of this on the emission

https://doi.org/10.1017/S1743921322001569 Published online by Cambridge University Press

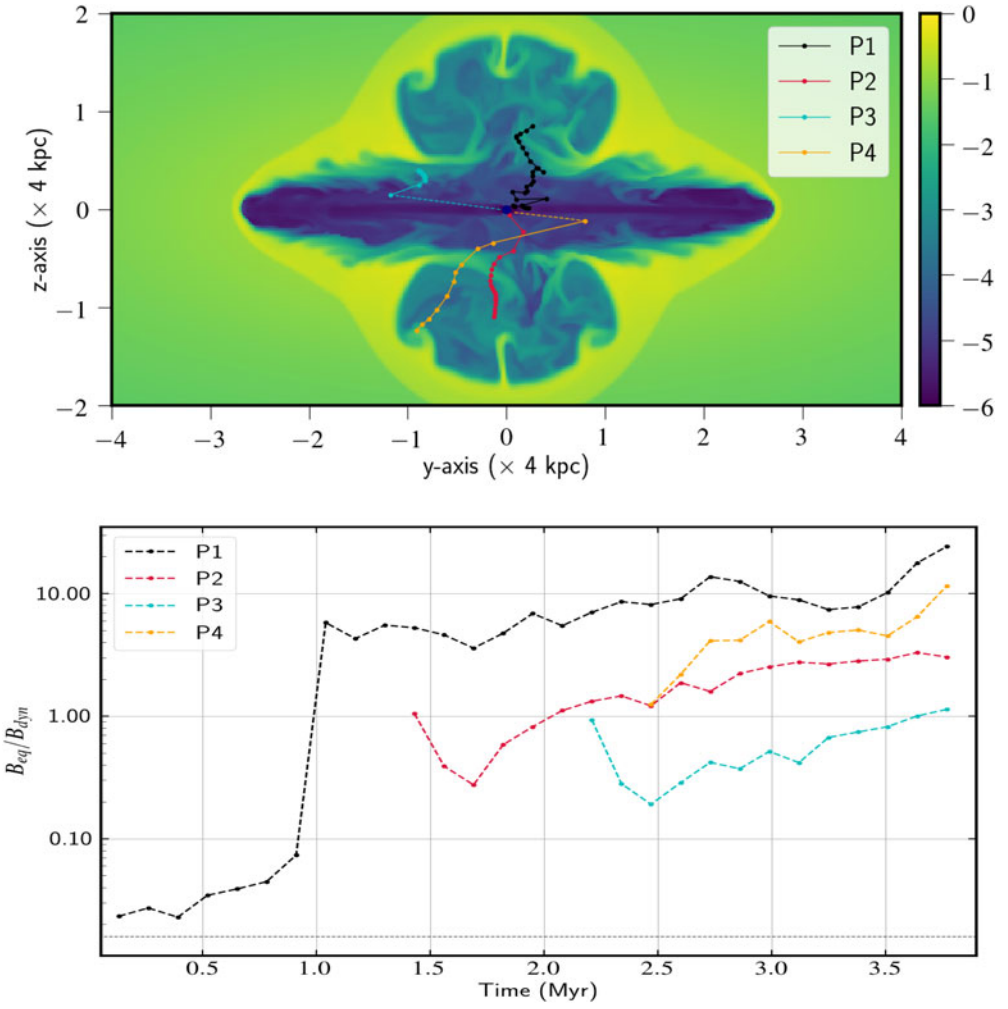

Figure 2. *Top: y-z* slice (at $x = 0$) of our simulated XRG (in 3D) at time 3.78 Myr, overplotted with the trajectories of four Lagrangian particles injected into the domain through the jet nozzle at different times. The corresponding colorbar represents the log variation of density of the galaxy. *Bottom:* evolution of $B_{\rm eq}/B_{\rm dyn}$ with time for the same particles where the dashed grey line represents the initial condition for the injected particles. A value of $B_{\rm eq} = B_{\rm dyn}$ indicates the true equipartition between the radiating electrons and the magnetic field of the galaxy.

signatures of wing and active lobe of XRGs have elaborately discussed by us in the study Giri et al. (2022).

One point to note here is that the trajectories of particles P1 and P2 do not contradict the ideal back-flow scenario. These particles were injected into the domain at a very early stage of the simulation when the wing-lobe structure was not prominent enough to distinguish. Moreover, the frequency of data saving of the simulation is also quite low for tracking the proper trajectories of these particles at their initial phase. Despite the fact, the changes in particle spectra concurrent to the micro-physical processes encountered by them are adequately captured, which is evident in Fig. 2 (bottom), where they show higher $\frac{B_{\rm eq}}{B_{\rm dyn}}$ values at their first detection than the initial injection condition.

The above discussion indicates that the equipartition condition of these radio galaxies varies with time as the particles evolve continuously under the cooling or re-energization

https://doi.org/10.1017/S1743921322001569 Published online by Cambridge University Press

processes in the turbulent cocoon and wing. An in-depth examination of the role of diffusive shocks and cooling in wing and lobe is discussed further in Giri et al. (2022). Here, in particular, we show that several particles alter their initial equipartition condition by shifting towards higher magnetic field ratios governed by the combined effect of the above mentioned micro-scaled processes. This indicates that the equipartition criterion of radio galaxies is not a ready to take assumption, and one must be careful in making its use in evaluating other physical parameters, for example, the spectral age of a radio galaxy (Mahatma et al. 2020; Giri et al. 2022).

5. Summary

We have performed high resolution 2D axi-symmetric and full scale 3D relativistic magneto-hydrodynamic simulation of jet propagation from triaxial galaxy to understand the formation of X-shaped radio galaxies based on the back-flow model. We affirm the role of pressure gradient of the ambient and hence the initial jet ejection direction in forming the X-shaped morphology as suggested by Capetti et al. (2002). In this case, the wing length is also governed by the magnetic field strength as strong fields tend to suppress the wing length due to stronger tension force. Further for our 3D simulations, we have adopted the model from Rossi et al. (2017) and have demonstrated the formation of X-shaped radio galaxies. We also show that older particles tend to accumulate in the wings, whereas lobes are mostly filled with freshly injected particles from the AGN.

Along with dynamical studies, we have also investigated the effect of back flow on the non-thermal particle spectral signatures of these galaxies which we have modelled using a hybrid approach considering the role of the diffusive shock acceleration (DSA) and the radiative and adiabatic cooling. We show that the role of DSA cannot be ignored in these galaxies as they keep the radio structure active during its evolution by re-accelerating particles against their drastic cooling. We have quantified the ratio of equipartition magnetic field $B_{\rm eq}$ with dynamical magnetic fields $B_{\rm dyn}$. During the course of evolution, the injected particles show a systematic shift from an initial sub-equipartition population $B_{\rm eq} < B_{\rm dyn}$ to approximately equipartition due to consistent evolution of particle distribution in presence of radiative losses from local magnetic fields and diffusive shock acceleration. This analysis indicates that equipartition between the radiating and magnetic energy is rather a dynamic process which evolves with time. Such an evolution has significant impact on the estimation of spectral age of radio galaxies as was demonstrated by Mahatma et al. (2020); Giri et al. (2022).

References

Capetti, A., Zamfir, S., Rossi, P., et al. 2002, A&A, 394, 39
Cavaliere, A. & Fusco-Femiano, R. 1976, A&A, 500, 95
Croston J. H., Hardcastle M. J., Harris D. E., et al. 2005, ApJ, 626, 733
Giri, G., Vaidya, B., Rossi, P., et al. 2022, A&A, DOI:10.1051/0004-6361/202142546
Gopal-Krishna Biermann P. L., Gergely L. Á., Wiita P. J., 2012, Research in Astronomy and Astrophysics, 12, 127
Hardcastle, M. J., Birkinshaw, M., Cameron, R. A., et al. 2002, ApJ, 581, 948
Hodges-Kluck E. J., Reynolds C. S., 2011, ApJ, 733, 58
Kraft R. P., Hardcastle M. J., Worrall D. M., Murray S. S., 2005, ApJ, 622, 149
Leahy, J. P. & Williams, A. G. 1984, MNRAS, 210, 929
Mahatma, V. H., Hardcastle, M. J., Croston, J. H., et al. 2020, MNRAS, 491, 5015
Mignone, A., Bodo, G., Massaglia, S., et al. 2007, ApJS, 170, 228
Mukherjee, D., et al. 2021, MNRAS [https://doi.org/10.1093/mnras/stab1327]
Rossi, P., Bodo, G., Capetti, A., & Massaglia, S. 2017, A&A, 606, A57
Vaidya, B., Mignone, A., Bodo, G., Rossi, P., & Massaglia, S. 2018, ApJ, 865, 144